JOURNAL OF MATERIALS SCIENCE 26 (1991) 2219–2228

Incommensurate modulated structure in the cubic–tetragonal transition of V–Ru alloys studied by high resolution electron microscopy

N. OHNISHI*, T. ONOZUKA, M. HIRABAYASHI‡
Institute for Materials Research, Tohoku University, Sendai 980, Japan

The cubic–tetragonal transition of V–Ru alloys near 50 at% has been investigated by high resolution transmission electron microscopy. In the cubic to tetragonal transition process of thin foil specimens, we found an incommensurate modulated structure showing satellite spots near $\frac{1}{4}\langle 0\,1\,1\rangle$ positions in the electron diffraction patterns. This incommensurate structure is composed of many domains of the commensurate modulated structure with a pseudo-tetragonal cell of $A = B = 2(a^2 + c^2)^{1/2}$ and $C = c$, where a and c ($\simeq 1.07a$) are the lattice constants of the tetragonally distorted CsCl-type structure. The modulation is interpreted in terms of the combination of dual elastic shear distortion waves nearly parallel to the $\langle 0\,1\,1\rangle$ directions with the approximate wavelength of $2\sqrt{2}a$. We propose a model for the incommensurate modulated structure.

1. Introduction

As is well known, some superconducting intermetallic compounds undergo a structural phase transition with decreasing temperature prior to the superconducting transition. Extensive studies have been done on this structural transition from both the theoretical and experimental points of view with particular attention to the correlation between the lattice instability and the superconducting transition [1]. The transition of these materials is described often as a weakly first-order martensitic transformation, which is characterized by a nearly continuous change of the degree of order of product phase and by precursor phenomena at temperatures above the transition point [2, 3]. An example is the cubic–tetragonal transition of Nb_3Sn and V_3Si with the A15 type structure [1–3]. The precursor phenomena in such a martensitic transformation is strongly correlated with the softening of the elastic modulus with decreasing temperature toward the transition point [2–4]. In the transmission electron microscopy (TEM) study, they are generally observed as fine-scale distorted microstructures, which appear in the matrix phase prior to the transition. These microstructures are accompanied by the extra spots or diffuse scattering in the electron diffraction pattern [4].

The $V_{50+x}Ru_{50-x}(x < 4)$ alloys, which have the cubic CsCl (B2) type structure in their high-temperature phase, undergo a structural transition to a tetragonal low-temperature phase with decreasing temperature. At the transition temperature T_m, remarkable changes take place in physical properties such as magnetic susceptibility and electrical resistivity. Following this transition, a superconducting transition occurs below T_m. The T_m decreases from 350 to 10 K with increasing vanadium concentration from 50 to 54 at% [5–8], while the superconducting critical temperature T_c rises correspondingly from below 1 to above 5 K. In view of the above properties, this transition has been investigated comparing with the A15 type superconductors. With X-ray diffraction and electrical resistivity measurements, this transition is found to be that of a weakly first-order [9, 10]. From calculations of the electronic band structure, the occurrence of internally modulated structures is expected in the tetragonal phase of V–Ru alloy [11].

We reported previously an *in situ* TEM study of the V–Ru alloys in the temperature range between 10 and 300 K [13, 14]. In the tetragonal phase of specimens near 50 at% V, we found two types of modulated structure showing extra reflection spots at the reciprocal lattice vector of $\boldsymbol{q} = \frac{1}{10}[1\,1\,2]$ and $\boldsymbol{q} \simeq \frac{1}{4}\langle 0\,1\,1\rangle$ in the electron diffraction patterns[§]. The $\frac{1}{4}\langle 0\,1\,1\rangle$ type modulated structure is incommensurate and appeared in thinner areas of the TEM specimens. It transforms to a commensurate structure with fine twinning at

* *Present address*: School of Materials Engineering, Purdue University, West Lafayette, Indiana 47907, USA.
‡ *Present address*: Kitami Institute of Technology, Kitami 090, Japan.
§ $\boldsymbol{q} = (1/x)[h\,k\,l]$ implies $\boldsymbol{q} = (h/x)\boldsymbol{a}^* + (k/x)\boldsymbol{b}^* + (1/x)\boldsymbol{c}^*$, where $\boldsymbol{a}^*$, $\boldsymbol{b}^*$ and $\boldsymbol{c}^*$ are the unit reciprocal lattice vectors for the tetragonally distorted CsCl-type structure, i.e. $|\boldsymbol{a}^*| = |\boldsymbol{b}^*|$.

0022–2461/90 $03.00 + .12

lower temperatures. On the other hand, the $\frac{1}{10}[1\,1\,2]$ type modulated structure is commensurate and is observed in relatively thick areas, where the accommodation of strain energy may play a leading role in forming the modulated structure. It is reasonable to consider, therefore, that the $\frac{1}{4}\langle 0\,1\,1\rangle$ type incommensurate modulation is a key for understanding the mechanisms of the cubic–tetragonal transition of V–Ru alloys. The aim of the present paper is to clarify the atomic arrangement of the $\frac{1}{4}\langle 0\,1\,1\rangle$ type incommensurate modulated structure and its microstructural relations with twins by means of high resolution transmission electron microscopy (HRTEM) and electron diffraction. Details of the $\frac{1}{10}[1\,1\,2]$ type modulated structure will be reported elsewhere.

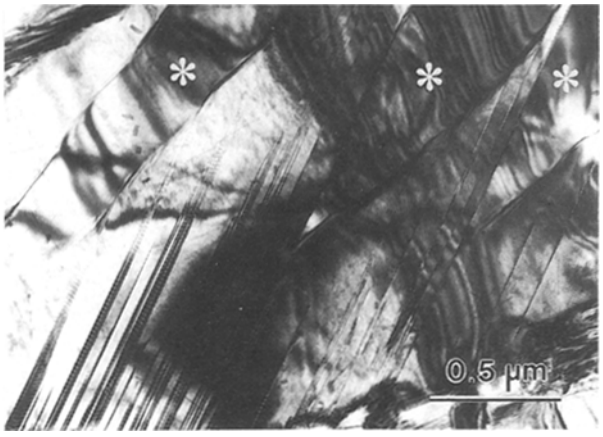

Figure 1 Bright field image of the tetragonal phase of 50.5 at % V alloy. Wedge-shaped areas marked with asterisks have the $\frac{1}{10}[1\,1\,2]$ type modulated structure.

2. Experimental procedures

Specimens of the V–Ru alloy containing 50.5 at % V were prepared by arc-melting in the atmosphere of high purity argon. This composition is favorable for the present study, because its transition temperature T_m is estimated to be around room temperature from the electrical resistivity measurement [5, 12]. For attaining compositional homogeneity, button ingots of 15 mm in diameter were remelted several times, and then annealed at 1900 K for 4 h in vacuum of 10^{-5} Torr. Discs of 0.3 mm thick and 2.3 mm in diameter were cut from these ingots, and annealed again at 1100 K and cooled slowly to room temperature. Thin foils for the TEM study were prepared by jet electrolytic polishing using an electrolytic solution of 300 ml H_2SO_4 and 700 ml CH_3OH. HRTEM observations were made at room temperature using a 200 kV electron microscope (JEOL 200CX) equipped with a top-entry goniometer. Fourier diffractograms of the HRTEM image were obtained from a digitalized data of the observed micrographs by using a computer-aided image processing system.

3. Experimental results

3.1. High resolution observation of the incommensurate modulated structure

Fig. 1 is a conventional TEM image of the 50.5 at % V alloy showing a transformed tetragonal structure. The

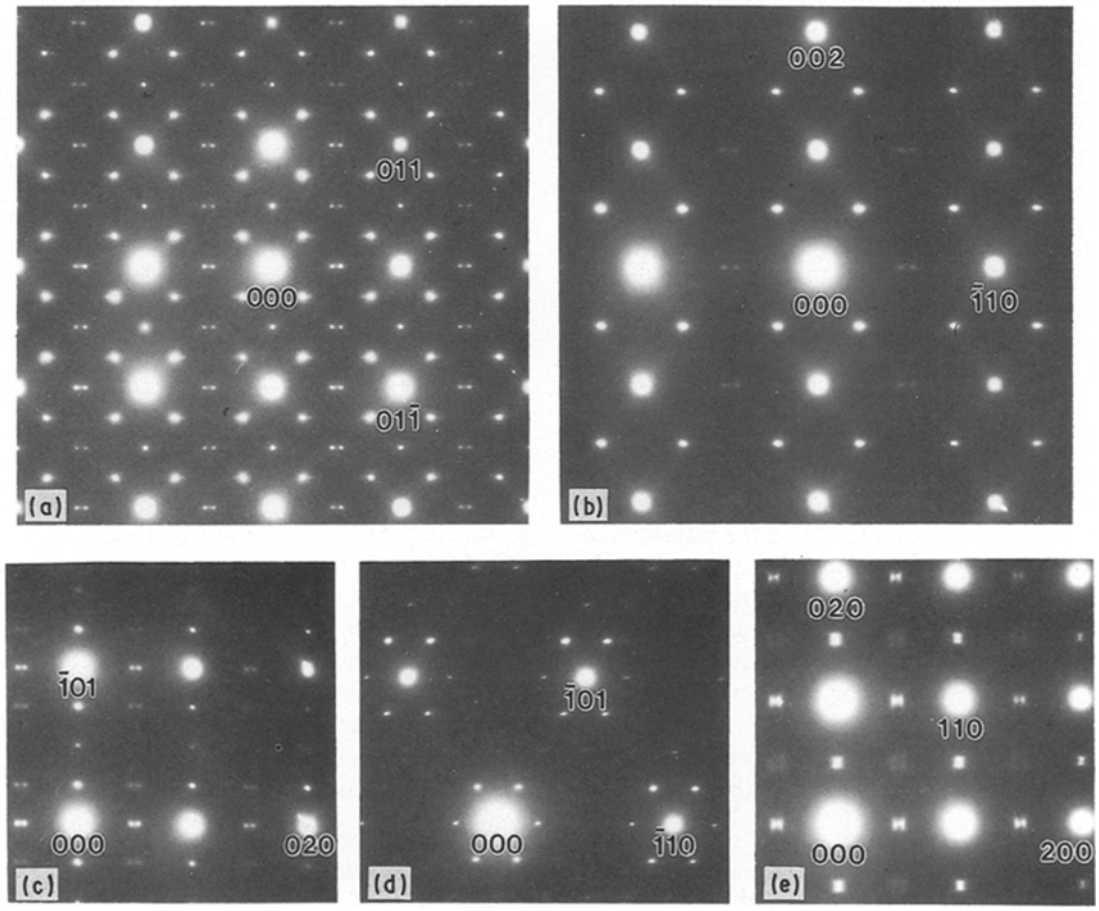

Figure 2 Selected area electron diffraction patterns of the $\frac{1}{4}\langle 0\,1\,1\rangle$ type modulated structure. Patterns a to e are taken under the [1 0 0], [1 1 0], [1 0 1], [1 1 1] and [0 0 1] incidences, respectively.

$\frac{1}{4}\langle 0\,1\,1\rangle$ type modulated structure is observed in the relatively thin area near the specimen edge in coexisting with the $\frac{1}{10}[1\,1\,2]$ type modulated structure at the thick areas marked with the asterisks. Fine twin lamellae parallel to the [0 1 1] direction exist in thin area. Selected area electron diffraction patterns of the $\frac{1}{4}\langle 0\,1\,1\rangle$ type modulated structure are shown in Fig. 2. The patterns of (a) to (d) are taken from the same area, whereas the pattern (e) is taken from a different area. A number of extra spots appear beside the fundamental reflections, which are analysed as the tetragonally distorted CsCl type structure with the axial ratio $c/a \simeq 1.07$.

The distribution of these extra spots in the reciprocal lattice is schematically illustrated in Fig. 3. The positions of the extra spots around each fundamental reflection are approximately expressed by combining the reciprocal lattice vectors $\boldsymbol{q} = \frac{1}{4}\langle 0\,1\,1\rangle$, as indicated by arrows. As shown in Fig. 3b, the extra spots are placed nearly parallel to, but slightly shifted from, the [0 1 1] rel-direction in the (1 0 0) rel-plane; i.e., they are in the "incommensurate" positions, being apparent as split spots in pairs. The reciprocal lattice vectors corresponding to these satellite spots are given as

$$\boldsymbol{q}_1 = \tfrac{1}{4}[0\,1\,1] - \boldsymbol{\delta}, \quad \boldsymbol{q}_2 = \tfrac{1}{4}[0\,\bar{1}\,1] + \boldsymbol{\delta}$$
$$\boldsymbol{\delta} \parallel [0\,1\,0] \qquad (1)$$

where the value of deviation vector $|\boldsymbol{\delta}|$ is estimated as about $0.016\,|\boldsymbol{a}^*|$ from the separation of the split spots. In addition to the above two vectors, other vectors such as that

$$\boldsymbol{q}_3 = \tfrac{1}{4}[1\,0\,1] - \boldsymbol{\delta} \quad \boldsymbol{q}_4 = \tfrac{1}{4}[\bar{1}\,0\,1] + \boldsymbol{\delta}$$
$$\boldsymbol{\delta} \parallel [1\,0\,0] \qquad (2)$$

exist in the (0 1 0) rel-plane.

Fig. 4 is a many-beam (HRTEM) image of the incommensurate modulated structure with the [1 0 0] incidence. The Fourier diffractogram inset, which is taken from a part of the image, shows the splitting of $0\frac{1}{2}0$ spots as marked by the arrows. This indicates the incommensurability of the modulation. The image consists of a large number of bright dots aligned in a fine square mesh, which corresponds to the projection of the tetragonally distorted CsCl unit cell; the periodic spacing of the bright dots along the two principal axes is equal to the cell constant a or c ($\simeq 0.3$ nm). In the image, we note brightness modulation of the dots forming a larger square mesh or checker pattern oriented nearly parallel to the [0 1 1] and [0 $\bar{1}$ 1] directions. The spacing of broad stripes in the checker pattern is approximately $4d_{(0\,1\,1)} = 2(a^2 + c^2)^{1/2}$ ($\simeq 0.85$ nm). The average direction of the stripes indicated by dashed lines is deviated slightly from the [0 1 1] or [0 $\bar{1}$ 1] direction in correspondence to the incommensurate feature of the electron diffraction pattern.

Fig. 5 shows an enlargement of a part of Fig. 4. In the image, we may recognize clearly fundamental cells of checker pattern having the dimension of $4d_{(0\,1\,1)}$ as marked by rhombuses. This result indicates that the incommensurate structure consists of many "domains" of the commensurate modulated structure

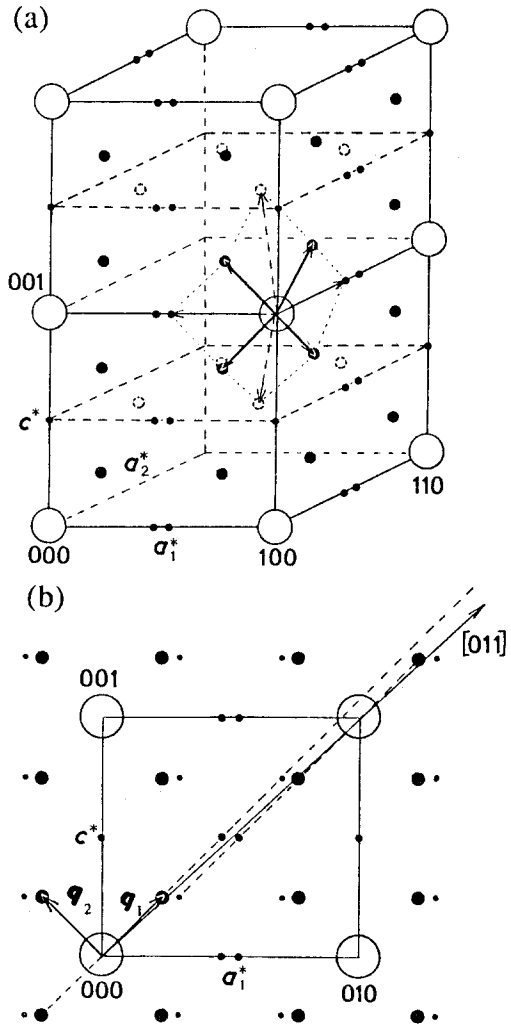

Figure 3 Schematic illustration of the distribution of extra spots in (a) the reciprocal lattice, and (b) on the (1 0 0) reciprocal lattice plane.

with the cell dimension of $4d_{(0\,1\,1)}$. In fact, we found a rather wide area of the commensurate structure as shown in Fig. 6. The bright dot alignment in the commensurate structure is highly "ordered" with the cell dimension of $4d_{(0\,1\,1)}$; i.e., the brightness modulation of the mesh pattern is oriented exactly parallel to the [0 1 1] and [0 $\bar{1}$ 1] directions. This image exhibits a single domain of the commensurate modulated structure, and the Fourier diffractogram inset shows no splitting of the $0\frac{1}{2}0$ spot; i.e., $\boldsymbol{q}_1 = \frac{1}{4}[0\,1\,1]$, $\boldsymbol{q}_2 = \frac{1}{4}[0\,\bar{1}\,1]$, and $|\boldsymbol{\delta}| = 0$. Such large domains of the commensurate structure are often observed around twin boundaries. It suggests that the growth of the domains occurs in the process of cubic tetragonal transition [14].

The fact that the incommensurate modulated structure is composed of many domains of the commensurate structure is also shown by the images with the [0 0 1] incidence. In Fig. 7, a modulation of the bright dot alignment appears with the spacing of $2a \simeq 0.6$ nm interleaving a less bright dot layer. We see that the alignments of brighter dot in the areas A and B lie along the [1 0 0] and [0 1 0] directions, respectively. This implies that the structure consists of two variants. In addition, we may observe out-of-step configurations of the brighter and less bright dot alignments in

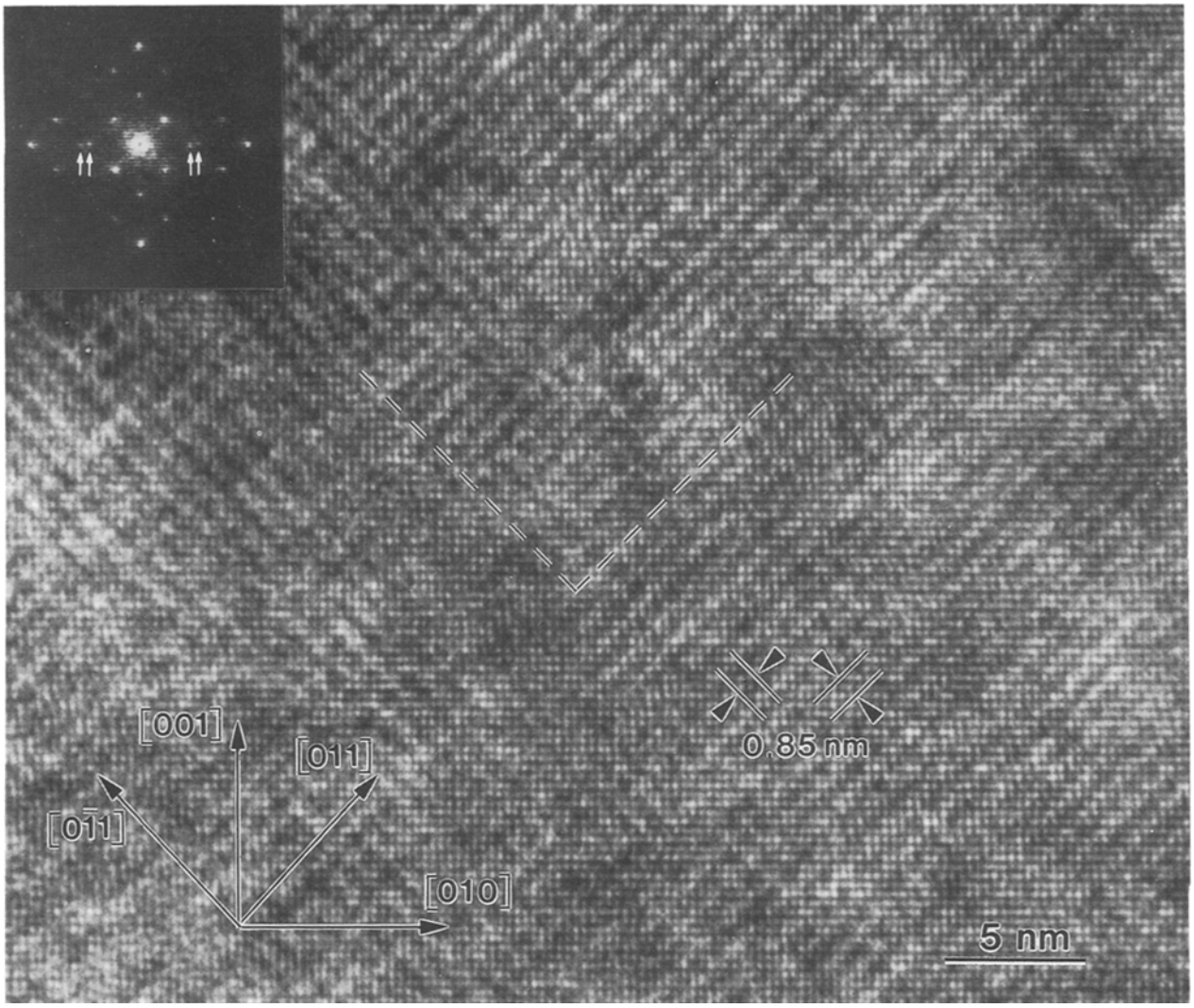

Figure 4 Many-beam image and its Fourier diffractogram of the $\frac{1}{4}\langle 0\,1\,1\rangle$ modulated structure. The incident beam is parallel to the [1 0 0] direction.

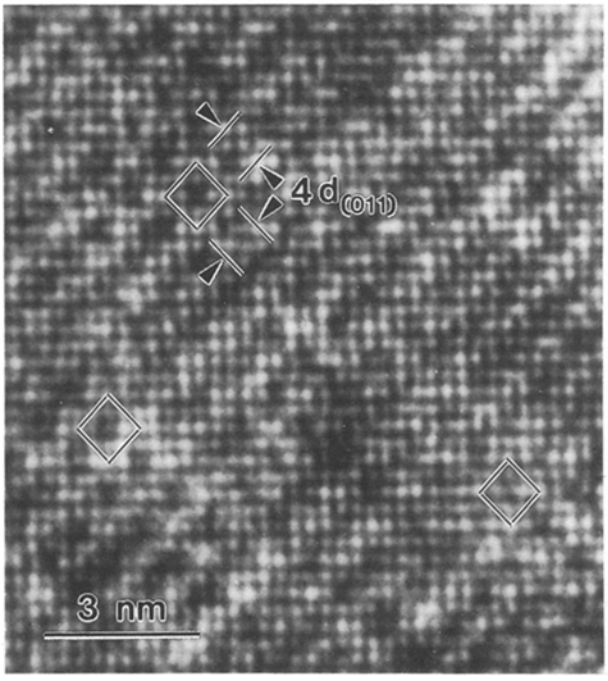

Figure 5 Enlargement of a part of Fig. 4. Rhombuses indicate a "fundamental cell" of the modulated structure.

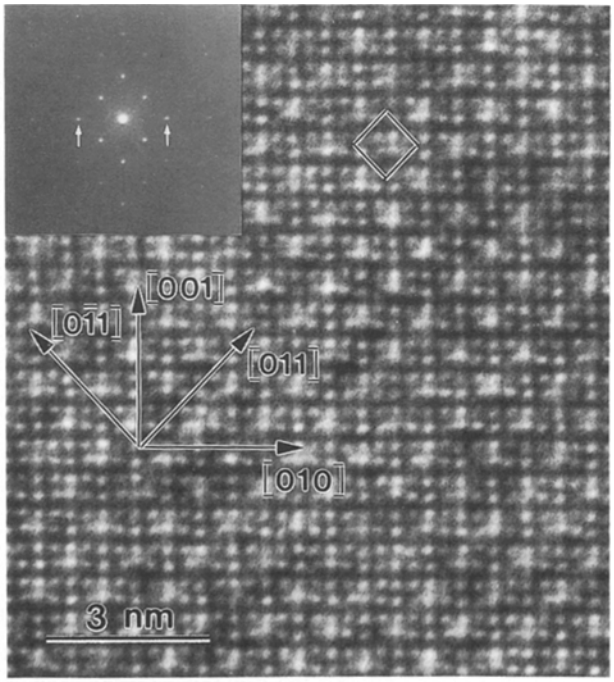

Figure 6 Many-beam image and its Fourier diffractogram showing a single domain of the commensurate modulated structure with the [1 0 0] incidence.

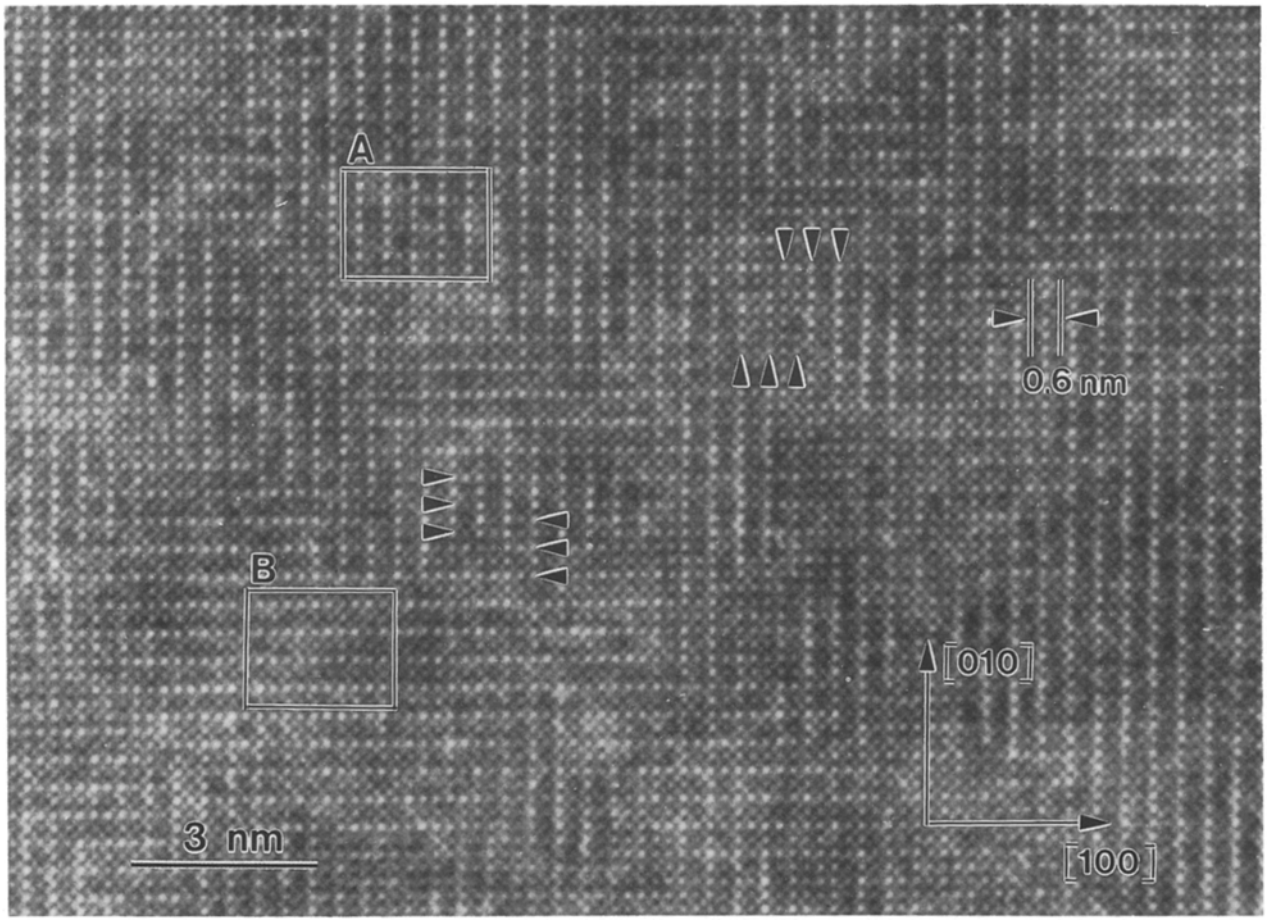

Figure 7 Many-beam image of the incommensurate modulated structure taken with the [0 0 1] incidence. Small arrows indicate the out-of-step configurations of two kinds of bright dot alignment.

both variants as indicated by the small arrows. This indicates that the incommensurate modulated structure of each variant is composed of many domains of the commensurate structure.

3.2. Fine twin structure with commensurate modulation

The microstructure of the lower temperature tetragonal phase is characterized commonly with fine twin lamellae lying parallel to the (0 1 1) plane. The fine twin structure was observed coexisting with the incommensurate modulated structure as shown in Fig. 1. Fig. 8 shows a many-beam image and an electron diffraction pattern of the twin structure, where the incident beam is kept parallel to the [1 0 0] direction. Fine twin lamellae consisting of alternating dark and bright band of 2 to 5 nm wide lie along the [0 1 1] direction, and strong streaks appear in the electron diffraction pattern along the direction perpendicular to the twin lamellae. Inside the twin lamellae, we see the chequered pattern of the modulated structure oriented exactly parallel to the $\langle 0\,1\,1 \rangle$ directions. It indicates that the modulated structure in the twin lamellae is commensurate.

An enlargement of a part of Fig. 8 is shown in Fig. 9. The c axes of the neighbouring twin lamellae indicated by large arrows are oriented nearly perpendicular to each other. In each twin lamella, we can see the commensurate modulated structure with the cell dimension of $4d_{(0\,1\,1)}$, although the contrast of the chequered pattern on one-side of the paired twin lamellae is not so obvious as on the other side. At the twin boundaries, the modulation of the bright dots is obscure over several layers of (0 1 1) planes, but the cell alignment of the commensurate modulated structure seems to be not connected coherently across the boundaries. We notice, furthermore, that there are out-of-step configurations of the bright dot alignments along both the a and c axes in every other lamellae, as indicated by small arrows, where the c axes have identical orientation. This feature observed between each twinned lamella is consistent with the split of extra spots along the exact [0 1 1] rel-direction in the electron diffraction pattern of Fig. 8. These results indicate that the commensurate modulated structure form twin lamellae with alternating crystallographic orientations and with a consistent phase shift of atomic arrangement across the twin boundaries.

4. Structural model and image simulation

The incommensurate modulated structure described above can be interpreted as being correlated with the $\{1\,1\,0\}$, $\langle 0\,\bar{1}\,1 \rangle$ type elastic shear distortion mode in the cubic to tetragonal transition. With the phenom-

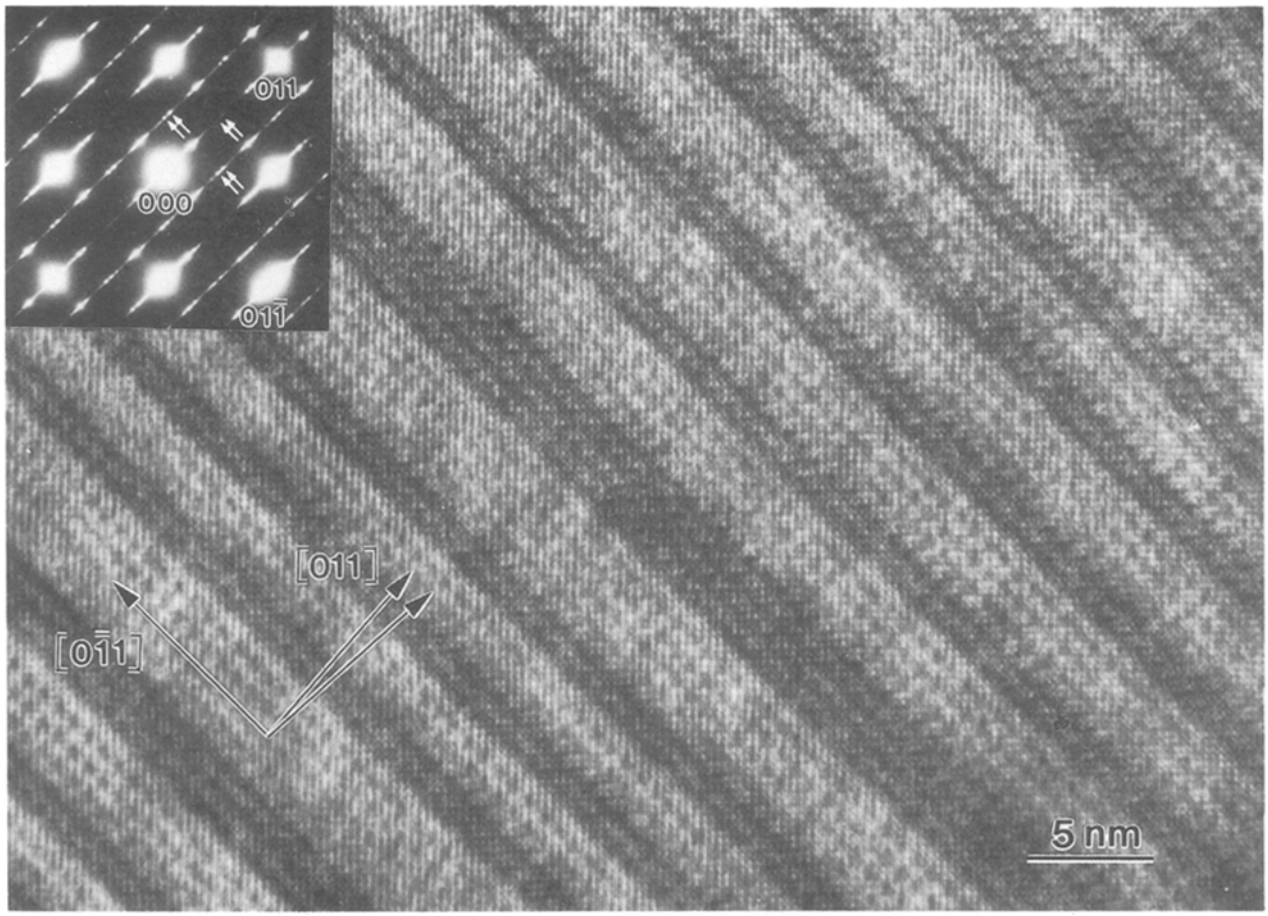

Figure 8 Many-beam image and electron diffraction pattern of twin structure. The incident beam is parallel to the [1 0 0] direction. Splitting extra spots in the electron diffraction pattern are marked by small arrows.

enological consideration, the displacement of atoms in the modulated structure is attributed to the combination of transverse displacement waves A_1 to A_4, the wavenumber vectors of which correspond to the reciprocal lattice vectors $\boldsymbol{q}_1$ to $\boldsymbol{q}_4$ of Equations 1 and 2, respectively. For instance, the component waves A_1 and A_2 on the (1 0 0) plane in the modulated structure represent dual transverse distortion waves lying approximately along the directions deviated slightly from the [0 1 1] and [0 $\bar{1}$ 1] with the wavelength nearly equal to $4d_{(0\,1\,1)}$, as illustrated in Fig. 10. The atomic positions on the plane of $x = 0$ (or $a/2$) are expressed as

$$\begin{aligned} y &= y_0 + (-d_1 + d_2)\sin\theta \\ z &= z_0 + (d_1 + d_2)\cos\theta \\ d_1 &= d_0 \sin[q_1(y_0\cos\theta + z_0\sin\theta)] \\ d_2 &= -d_0\sin[q_2(y_0\cos\theta - z_0\sin\theta)] \\ \tan\theta &= 2c/(2a + \Delta) \end{aligned} \quad (3)$$

where y_0 and z_0 are the original coordinates of the metal atoms, q_1 and q_2 the value of the wavenumber vectors $\boldsymbol{q}_1$ and $\boldsymbol{q}_2$ ($q_1 = q_2 = 2\pi/[(2a + \Delta)^2 + (2c)^2]^{1/2}$), and d_0 the amplitude of the waves. The parameter Δ is the deviation from the [0 1 1] and [0 $\bar{1}$ 1] direction as shown in Fig. 10, being proportional to the value $|\delta|$. Here, it should be noted that the waves are deviated along the [0 1 0] direction being consistent with the electron diffraction patterns. The waves A_3 and A_4 on the (0 1 0) plane, which correspond to $\boldsymbol{q}_3$ and $\boldsymbol{q}_4$, are expressed in a similar way.

On the basis of the results of high resolution observation, we consider first about a modulation derived from the pair of waves A_1 and A_2. Fig. 11a is a schematic illustration of the atomic arrangement of the modulation projected on the (1 0 0) plane, where open and closed circles correspond to the vanadium and ruthenium atoms, respectively. In this model, the deviation parameter is neglected, i.e., $\Delta = 0$ in Equations 3, and hence, a large square of thick lines corresponds to the unit cell of the commensurate modulated structure, which is shown in the image of Figs 5 and 6. It has pseudo-tetragonal* cell of axial length $A = B = 4d_{(0\,1\,1)} = 2(a^2 + c^2)^{1/2}$ and $C = a$. In the atomic arrangement of the modulated structure derived from combining the dual transverse waves, four subcells of thin lines are symmetrically rotated around the [1 0 0] axis as marked by the arrows.

Fig. 11b shows the projection of this atomic arrangement along the [0 0 1] direction. We see here that the projected atomic arrangement has the periodic spacing of $2a$ along the [0 1 0] direction which is consistent with the observed image of Fig. 7. It shows that the two variants of the bright dot alignment

*To be accurate, the axial angle γ is given as $2\tan^{-1}(c/a)$ ($\neq 90°$).

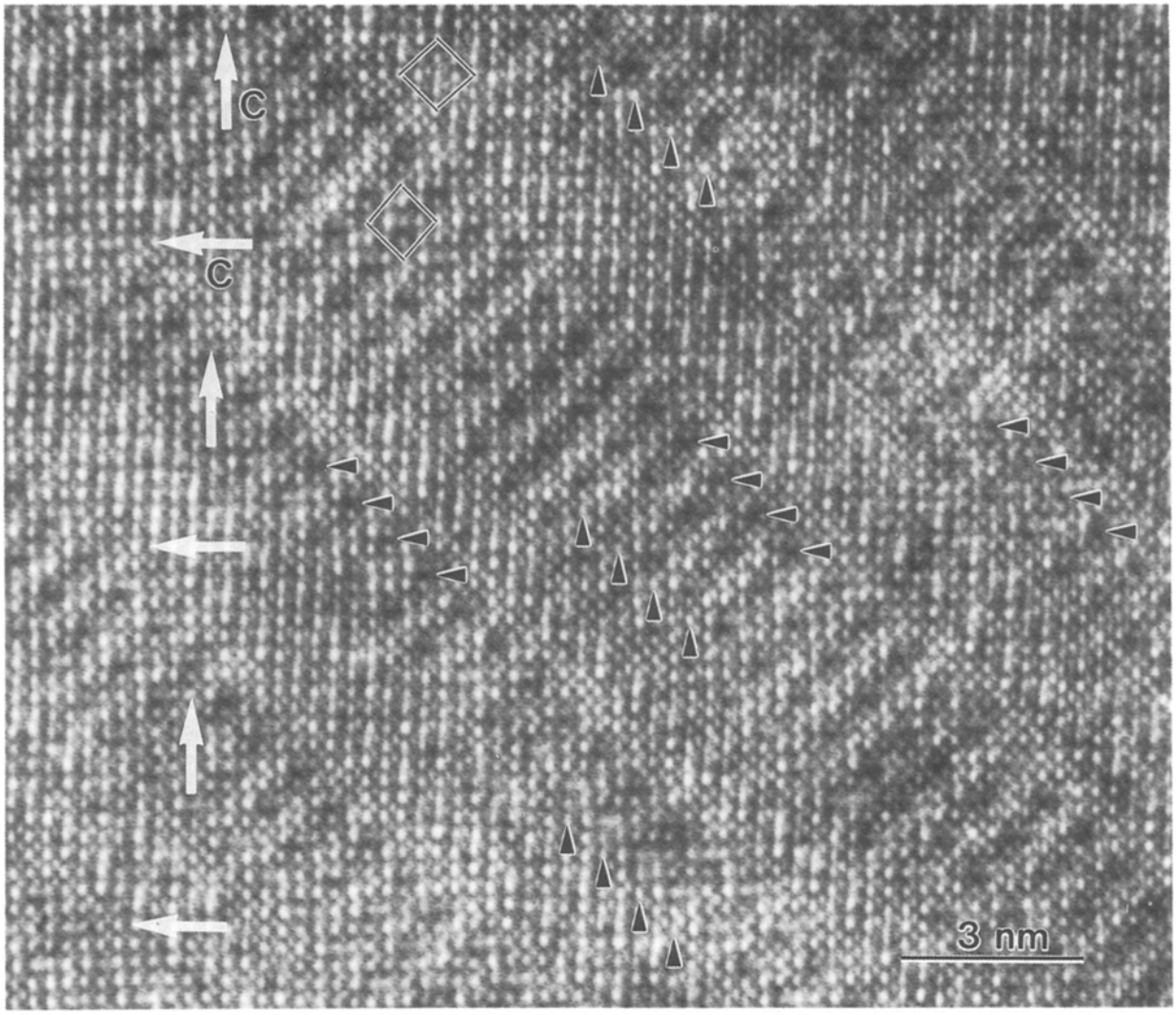

Figure 9 Enlargement of a part of Fig. 8. Alternating changes of the c-axis are indicated by large arrows. Small arrows indicate out-of-step configurations of the bright dot alignment.

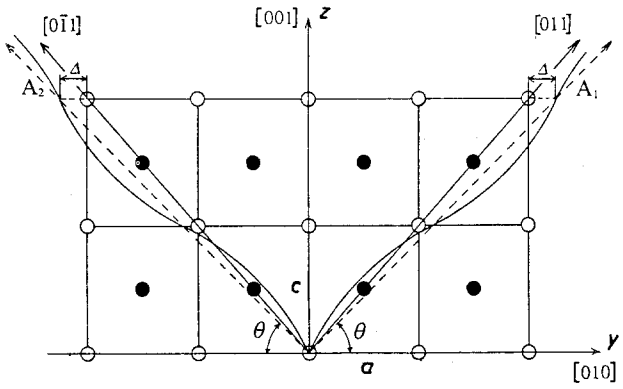

Figure 10 Schematic illustration of the transverse displacement waves A_1 and A_2 on the (1 0 0) plane. Open and closed circles represent vanadium and ruthenium atoms, respectively.

(areas A and B in Fig. 7) correspond to the modulated structure with the paired waves of $A_1 + A_2$ on the (1 0 0) plane and that with $A_3 + A_4$ on the (0 1 0) plane.

In order to obtain faithful interpretation of the observed many-beam image, we carried out image calculations based on the commensurate modulated structure ($\Delta = 0$) of Fig. 11. In Fig. 12, series of the simulated images by the multi-slice method are shown as a function of the defocus value Δf and the specimen thickness t. Parameters used for the computation are listed in Table I. The amplitude d_0 of the shear distortion waves, which is exaggerated in Figs 10 and 11, is assumed to be 1% of a. In the simulated images, the atomic displacement is enhanced because of the dynamical scattering effect of electrons propagating through the slices. The chequered patterns of the brightness modulation observed in Figs 5 and 6 are well reproduced in the calculations of Fig. 12a, although the contrast reverse takes place with changing the defocus and the thickness. From comparison with the calculated images, the displacement amplitude d_0 of 1 to 2% gives the best fitting to the experimental results. In the simulated images of Fig. 12b, the brightness modulation with the periodic spacing $2a$ along the [0 1 0] direction in Fig. 7 is well reproduced at the Scherzer defocus $\Delta f = 50$ nm and thickness $t = 31$ nm.

Next, to compare with the electron diffraction patterns, we calculated kinematical diffraction intensity on the basis of the structure model for the incommensurate modulation taking account of the deviation Δ and the four waves A_1 to A_4 on the (1 0 0) and (0 1 0) planes. The atomic positions of the structure model

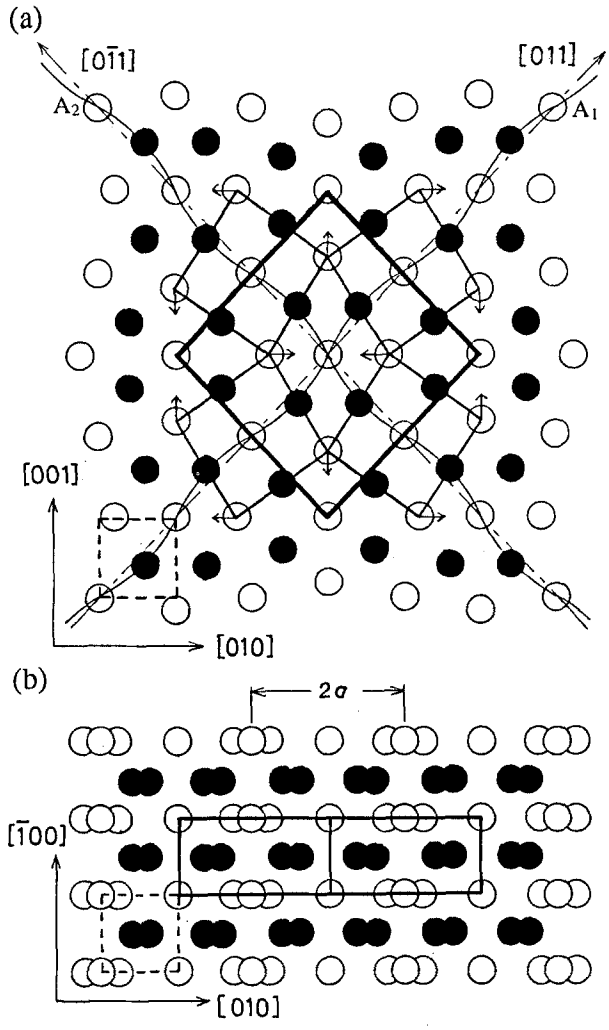

Figure 11 Atomic arrangement projected on the (1 0 0) (a) and (0 0 1) (b) planes of the commensurate modulated structure. Small squares with dashed lines indicate the unit cell of tetragonally distorted CsCl type structure.

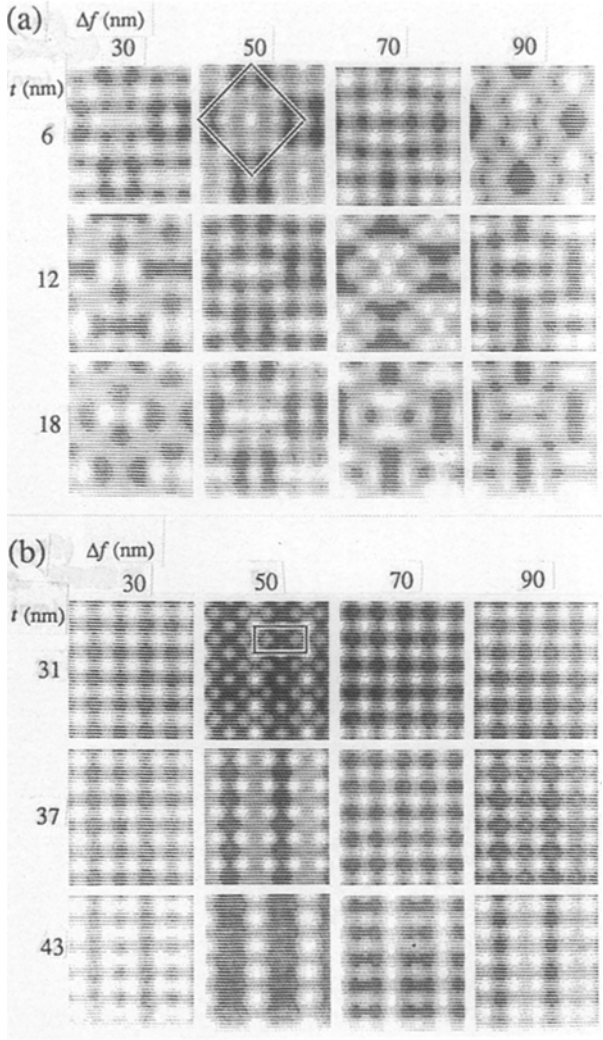

Figure 12 Series of simulated images for the commensurate modulated structure. [1 0 0] (a) and [0 0 1] (b) projections are shown as functions of crystal thickness t and defocus values Δf. The unit cells are outlined in (a) and (b).

are derived by an extension of Equations 3 to include the additional two waves A_3 and A_4. It gives homogeneous modulation of atoms which does not yield the commensurate domains. In the calculation, we assumed that the lattice dimension of the incommensurate structure model is $30a \times 30a \times 4c$ ($\Delta = 2a/30$) of the fundamental tetragonal cell, and the displacement amplitude d_0 is 2% of a. The results on the (1 0 0), (1 1 0), (1 0 1), (1 1 1) and (0 0 1) rel-planes are shown in Fig. 13. All the spots in the observed electron diffraction patterns of Fig. 1a to e are well reproduced by the calculations.

TABLE I Parameters used for the image computation

Wavelength (nm)	0.0251
Spherical aberration coefficient (mm)	0.8
Objective aperture radius (nm^{-1})	8
Crystal thickness for one slice (nm)	0.287 ([1 0 0] incidence) 0.307 ([0 0 1] incidence)
Defocus due to chromatic aberration (nm)	13
Number of beams	32 × 32

5. Discussion

The above results indicate that the formation of the $\frac{1}{4}\langle 0\,1\,1\rangle$ type incommensurate modulated structure of V–Ru alloy is attributed to the lattice instability of the CsCl type structure prior to the cubic–tetragonal transition, and is derived by combining the lattice distortion waves A_1 to A_4 along the directions deviated slightly from $\langle 1\,1\,0\rangle$. The observed TEM images show that the incommensurate modulated structure consists of numerous domains of the commensurate structure, which is expressed by the two-dimensional modulation due to the two variants of paired waves $A_1 + A_2$ or $A_3 + A_4$ with $\Delta = 0$.

In Fig. 14, we present a schematic model of the incommensurate modulated structure composed of the domains of the commensurate modulated structure. This shows a plausible atomic arrangement of the incommensurate modulated structure in a single variant region, where, open circles indicate the projected position of vanadium (or ruthenium) atoms, and rhombuses of thin lines correspond to the unit cell of the commensurate modulated structure with the dimension of $4d_{(0\,1\,1)}$. Neighbouring domains of commensurate structure are assumed to lie parallel to the

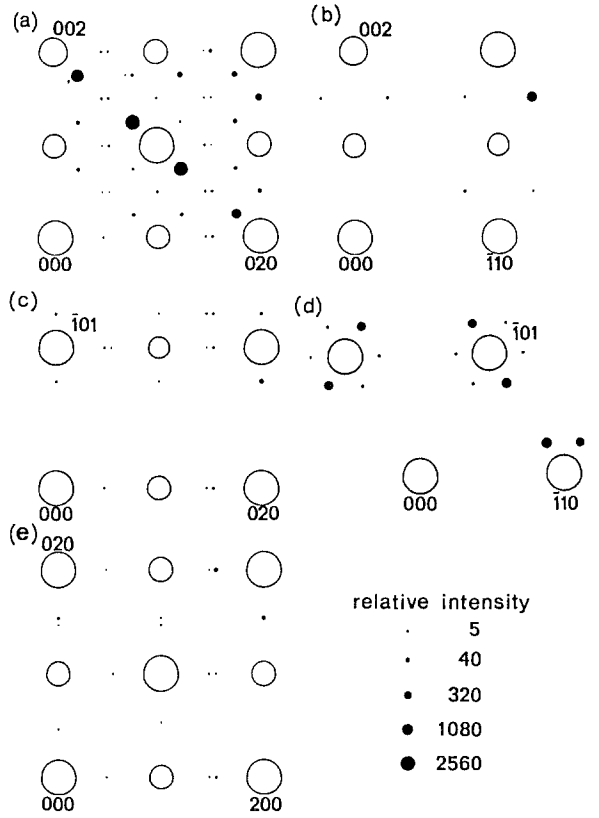

Figure 13 Kinematical intensity distributions calculated from a model of three-dimensional incommensurate modulated structure. The patterns (a) to (e) correspond to the results on the (1 0 0), (1 1 0), (1 0 1), (1 1 1) and (0 0 1) rel-planes, respectively. The relative intensity of extra spots is indicated.

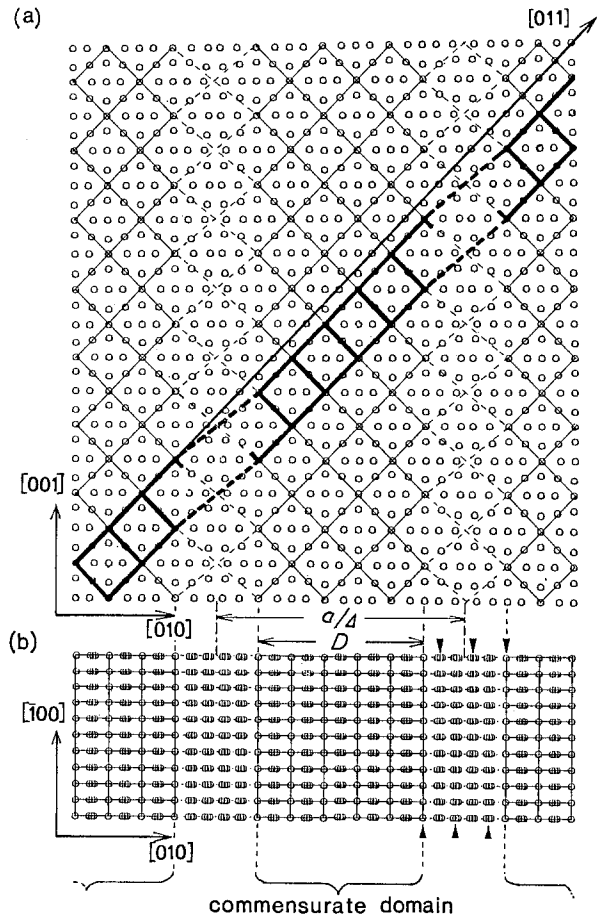

Figure 14 Schematical model of the incommensurate modulated structure composed of domains of the commensurate modulated structure. Ruthenium atom positions are not shown.

(0 1 0) plane so as to be consistent with the orientation of the deviation vector δ obtained from the electron diffraction patterns. The modulation period is, therefore, incommensurate along the [0 1 0] direction, but commensurate along the [0 0 1] direction, even though the distortion waves are oriented along the $\langle 0\,1\,1\rangle$ directions. We may call it a partially incommensurate structure as proposed by Yamada [15]. The interval of domain is given by a/Δ, whereas their width D may vary arbitrarily from 0 to a/Δ. The phase shift of atomic position between neighbouring domains is taken as $\pi/2$ in order to have the average position of atoms expressed by Equations 3 ($\Delta \neq 0$). An alignment of the rhombuses indicated by thick lines, which correspond to the broad stripes of the mesh pattern observed in Figs 4 and 5. A series of kinks are formed at the domain boundary regions and hence the average direction of the alignment deviates from the [0 1 1] direction. A projected view of the model along the [0 0 1] direction is illustrated in Fig. 14b. It shows the out-of-step configurations between the neighbouring domains as indicated by the small arrows being consistent with the brighter dot alignment observed in Fig. 7. The above model can explain well the characteristic features of the observed HRTEM images and electron diffraction patterns.

Finally we shall discuss the cubic–tetragonal transition process of the V–Ru alloy on the basis of the above results. At the initial stage of the transition, the four distortion waves A_1 to A_4 may contribute equally to a homogeneous structural modulation. Subsequently two variants of the incommensurate modulation are nucleated randomly by coupling the dual distortion waves $A_1 + A_2$ or $A_3 + A_4$, which might be caused by local fluctuation of lattice distortion. Then the growth of the commensurate domains occurs in the incommensurate modulated structure during the process of the cubic–tetragonal transition. In this growth process, the deviation vector δ in the reciprocal space is kept along the [0 1 0] (or [1 0 0]) rel-direction; i.e., the commensurate domains are aligned along the [0 1 0] (or [1 0 0]) direction as illustrated in Fig. 14.

With further lowering temperature, the growth of the commensurate domain is accompanied by the formation of fine twin lamellae [14], to accommodate the elastic strain energy accumulated with the gradual increase of the tetragonal distortion [10]. The observed images show that the twin structure consists of an array of the commensurate structure, the atomic arrangement of which has a regular out-of-phase relation across the twin boundaries. In other words, the twin structure is a systematic alignment of the commensurate domains along the [0 1 1] direction, that is to say, the twinning process in this transition accommodates the tetragonal distortion by rearranging the commensurate domains which are contained in the incommensurate modulated structure.

6. Summary

High resolution electron microscopy on the incommensurate modulated structure in the cubic–tetra-

gonal transition of V–Ru alloy has been carried out. The results obtained in the present study are summarized as follows:

(1) The incommensurate modulated structure consists of numerous commensurate domains with a pseudo-tetragonal unit cell of $A = B = 2(a^2 + c^2)^{1/2}$ and $C = a$, where a and c are the lattice constant of the tetragonally distorted CsCl-type structure. The domains grow as the cubic–tetragonal transition proceeds.

(2) The atomic arrangement in the commensurate modulated structure is proposed by combining the coupling of dual elastic distortion waves along the $\langle 0\,1\,1 \rangle$ directions on the (1 0 0) (or (0 1 0)) plane. Satisfactory agreement is obtained between the observed high resolution electron micrographs and the calculated images based on the proposed model.

(3) The incommensurability of the modulated structure is explained by accounting a systematic distribution of the commensurate domains along the [0 1 0] (or [1 0 0]) directions. It corresponds to the modulation caused by the pair of distortion waves slightly shifted from the $\langle 0\,1\,1 \rangle$ directions.

(4) The twin structure, which succeeds the incommensurate modulated structure, is composed of an array of lamellae with the commensurate modulated structure lying parallel to the (0 1 1) planes. It is suggested that the twinning process is responsible for the rearrangement of the commensurate domains contained in the incommensurate structure.

Acknowledgements

We are grateful to Professor K. Hiraga in our institute and Professor H. Sato in Purdue University for their useful discussions. This work was supported partly by the Grant-in-Aid for Scientific Research from the Ministry of Education, Science and Culture. One of us (N.O.) wishes to acknowledge a Fellowship of the Japan Society for Promotion of Science for Japanese Junior Scientists.

References

1. L. R. TESTARDI, *Rev. Mod. Phys.* **47** (1975) 637.
2. N. NAKANISHI, in "Progress in Materials Science" Vol. 24, edited by J. W. Christian, P. Haasen and T. B. Massalski, (Pergamon, New York, 1980) p. 143.
3. N. NAKANISHI, A. NAGASAWA and Y. MURAKAMI, *J. Physique* **43** (1982) 35.
4. L. E. TANNER and W. A. SOFFA (eds), *Met. Trans.* **A19** (1988), 159–234, 761–820.
5. C. W. CHU, E. BUCHER, A. S. COOPER and J. P. MAITA, *Phys. Rev.* **B4** (1971) 320.
6. M. MAREZIO, P. D. DERNIER and C. W. CHU, *ibid.* **B4** (1971) 2825.
7. L. B. WELSH and C. W. CHU, *ibid.* **B8** (1973) 1026.
8. T. TSUKAMOTO, K. KOYAMA, A. OOTA and S. NOGUCHI, *J. Phys.* **F17** (1987) 1695.
9. A. OOTA and J. MULLER, in Proceedings of the International Conference on Martensitic Transformations, Nara, August 1986, edited by I. Tamura (Japan Institute of Metals, Sendai, 1986) p. 1121.
10. *Idem., J. Phys.* **F17** (1987) 153.
11. T. ASADA, T. HOSHINO and M. KATAOKA, *ibid.* **F15** (1985) 1497.
12. A. OOTA, M. TSUCHIYA and S. NOGUCHI, *ibid.* **F14** (1984) 899.
13. N. OHNISHI, T. ONOZUKA and M. HIRABAYASHI, in Proceedings of the MRS International Meeting on Advanced Materials, Vol. 9, Tokyo, June 1988, edited by K. Otsuka and K. Shimizu (Materials Research Society, Pittsburgh, 1988) p. 531.
14. N. OHNISHI, T. ONOZUKA and M. HIRABAYASHI, in Proceedings of the International Conference on Martensitic Transformations, Sydney, July 1989, edited by B. C. Muddle, Materials Science Forum, Vol. 56–58 (1990) p. 83.
15. Y. YAMADA, *Phys. Rev.* to be published.

Received 5 March
and accepted 9 March 1990